Fine-grained analysis of reconfigurable intelligent surface-assisted mmWave networks

Fine-Grained Analysis of Reconfigurable Intelligent Surface-Assisted mmWave Networks

Le Yang*, Xiao Li*, Shi Jin*, Michail Matthaiou†, and Fu-Chun Zheng*‡
*National Mobile Communications Research Laboratory, Southeast University, Nanjing, China
†Centre for Wireless Innovation, Queen's University Belfast, Belfast BT3 9DT, U.K.
‡School of Electronic and Information Engineering, Harbin Institute of Technology (Shenzhen), Shenzhen, China
Emails: {yangle, li_xiao, jinshi}@seu.edu.cn m.matthaiou@qub.ac.uk, fzheng@ieee.org

***Abstract*—Reconfigurable intelligent surfaces (RISs) have emerged as a promising technology for the next generation networks. By utilizing tools from stochastic geometry, we develop a meta distributed-based analytical framework to study the effect of the large-scale deployment of the RIS on the performance of a millimeter wave (mmWave) cellular network. Specifically, the locations of the base stations (BSs) are modeled as Poisson point processes (PPPs). In addition, the blockages are modeled by a Boolean model and a fraction of the blockages are coated with RISs. By considering the randomness of the locations and orientations of the RISs and the particular characteristics of mmWave communications, we provide a statistical characterization of the path loss for the BSs and RISs and derive the analytical expressions for the k-th moment of the conditional success probability, the area spectral efficiency and the energy efficiency. Numerical results demonstrate that better coverage performance and higher energy efficiency can be achieved by a large-scale deployment of RISs.**

***Index Terms*—Millimeter wave, reconfigurable intelligent surfaces, stochastic geometry.**

I. Introduction

The evolution of existing mobile applications and the constantly emergence of new applications have led to an explosive growth of the wireless data traffic. Millimeter wave (mmWave) communication stands out as a promising method to meet the data demand due to the abundant spectrum [1]. However, the high path loss and poor penetration into buildings prohibit the mmWave networks from providing universal coverage. Fortunately, reconfigurable intelligent surface (RIS), a surface consisting of a large number of reflective elements, provides an energy efficient approach to increase the coverage while creating a customized electromagnetic propagation environment by manipulating electromagnetic waves[2].

The RISs can be utilized in various application scenarios [3], [4], such as physical layer security enhancement [6], energy efficiency improvement and spatial modulation [7]. The results in [8] confirmed the huge potential of RISs to enhance the secrecy performance. The work of [9] demonstrated that the secrecy rate of an RIS-assisted wireless communication system can be enhanced by utilizing artificial noise. In [10], the base station (BS) transmit beamforming and RIS reflective beamforming were optimized jointly to maximize the minimum secrecy rate of the RIS-assisted networks under the assumption of discrete and continuous RIS phase shifts. The success probability of RIS-assisted networks was investigated in [11]-[12]. Exploiting the Boolean model, In [11], the achievable rate and energy efficiency were derived for RIS-assisted millimeter networks. In [12], the authors derived the ratio of the blind spots to the entire area and the distribution of the path loss between the typical user and its serving BS.

However, the existing works leverage the success probability as a key performance metric, which is defined as the probability of the signal-to-interference-plus-ratio (SINR) exceeding a pre-defined threshold T, i.e., $\mathbb{P}[\text{SINR} > T]$, given a spatial realization of BSs and users. The success probability is obtained by averaging the conditional success probability (a random variable) over the BS realizations and channel fading, from which the SINR variations across the individual links cannot be characterized. In order to obtain a fine-grained analysis on the SINR distribution of the RIS-assisted networks, inspired by [13], we herein adopt the meta distribution of the SINR as the performance metric. This is defined as the complementary cumulative distribution function (CCDF) of the conditional success probability. In other words, the success probability only answers the question of "On average, what fraction of users experience successful transmission (i.e., SINR $> T$)?". The meta distribution answers the question "What fraction of users can achieve the conditional success probability of at least y (an arbitrary percentage value)?". By considering the randomness for the location and orientation of the RISs, we provide a statistical characterization of the RISs and BSs in the mmWave networks with the Boolean modeled blockages. The RIS utilization is also provided, which is the fraction of the RISs that are actually being utilized to provide reflected links. The main contributions of the work are summarized as follows:

1) We develop a meta distribution-based framework to analyze the performance of a RIS-assisted mmWave cellular network by modeling the distributions of the

The work was supported in part by the National Key R&D Program of China under Grants 2020YFB1805005 and 2021YFB2900304, the Shenzhen Science and Technology Program under Grant KQTD20190929172545139, the NSFC under Grant 61941104, the Key Research and Development Program of Shandong Province under Grant 2020CXGC010108, the NSFC under Grant 61971126, the Natural Science Foundation of Jiangsu Province under Grant BK20211511 and the European Research Council (ERC) under the European Union's Horizon 2020 research and innovation programme under Grant 101001331.

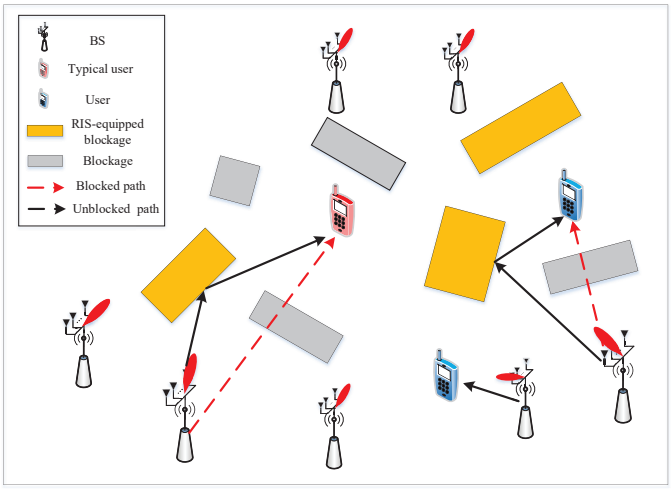

Figure 1. The layout of a RIS-assisted mmWave network.

BSs and RISs as Poisson point processes (PPPs). The distributions of the distance between the typical user and its serving BS/RIS are obtained. Based on the results, the k-th moment of the conditional success probability for the RIS-assisted mmWave cellular network is obtained. Moreover, analytical expressions of the mean local delay, ASE and energy efficiency are presented.

2) The simulation results demonstrate the impact of the key network parameters, such as the density of the BSs/RISs and the size of RISs, on the SINR meta distribution, mean and variance of the conditional success probability and energy efficiency. Simulation results for the traditional networks without RISs are also provided for the sake of comparison.Our conclusion is that RISs can effectively improve the success probability of the mmWave networks.

II. System Model

We consider a RIS-assisted mmWave cellular network, as shown in Fig. 1. The locations of the BSs and users are assumed to follow independent PPPs Φ_B and Φ_U with density λ_B and λ_U, respectively. Each BS and user are equipped with a ULA and the number of antennas at the BSs and users are denoted by N_B and N_U, respectively. Let P denote the transmit power of each BS. The available bandwidth is denoted by W (in Hz). We assume that a fraction of the blockage is coated with RISs and the RISs are distributed according to a PPP Φ_R with density λ_R. The number of the elements on the RIS is denoted by N_R. Without loss of generality, according to Slivnyak's theorem [14], we can study the performance of the typical user u_0 located at the origin $o \in \mathbb{R}$.

Since all BSs operate in the mmWave frequency, the communication link is sensitive to blockage effects. The link between u_0 and an arbitrary BS can be either LOS or NLOS, which is dependent on the visibility of the BS to u_0. If there are no blockages between u_0 and the BS, the corresponding link is LOS. Otherwise, the link is considered to be NLOS. The LOS probability of the link between u_0 and an arbitrary BS at distance x is defined by a LOS probability function, i.e., $p_L(x) = e^{-\beta x}$, where the blockage parameter β is dependent on the densities of the BSs and blockages [14]. The NLOS probability of the corresponding link, i.e., $p_N(x)$, is therefore $1 - e^{-\beta x}$.

The signal received by u_0 is attenuated by the path loss, and the severity of the attenuation can be measured by the path loss exponent. To distinguish the LOS/NLOS states of the link, different path loss laws are applied to the links under the LOS/NLOS link states. Therefore, the path loss is given by

$$L(x) = \begin{cases} \kappa_L x^{\alpha_L} & \text{with probability } p_L(x) \\ \kappa_N x^{\alpha_N} & \text{with probability } p_N(x), \end{cases} \tag{1}$$

where κ_L and κ_N are the path losses of the LOS/NLOS links at the reference distance of 1 meter, while α_L and α_N represent the path loss exponents of the LOS and NLOS links, respectively. Note that the signal is spatially sparse in the angle domain and the multipath components originate mainly from reflections rather than scattering and refraction [15]-[17]. Therefore, we neglect small-scale fading hereafter.

There are two types of channels for the typical user, i.e., the direct channel and the reflected channel. The direct channel denotes the channel between the typical user u_0 and its serving BS. The channel of the direct link between u_0 and the serving BS can be expressed as

$$\mathbf{H}_{i_0,0} = \mathbf{a}_{N_U}(\phi_{i_0,0})\mathbf{a}_{N_B}^{\mathrm{H}}(\theta_{i_0,0}), \tag{2}$$

where the vectors $\mathbf{a}_{N_U}(\phi_{i_0,0})$ and $\mathbf{a}_{N_B}(\theta_{i_0,0})$ are

$$\mathbf{a}_{N_U}(\phi_{i_0,0}) = \frac{1}{\sqrt{N_U}}[1, e^{j2\pi\phi_{i_0,0}}, \cdots, e^{j2\pi(N_B-1)\phi_{i_0,0}}]^{\mathrm{T}}, \tag{3}$$

where $i_0 \in \Phi_B$ is the index of u_0's serving BS, $\phi_{i_0,0} = d\cos\varphi_{i_0,0}/\omega$ is the normalized AoA at u_0 and $\theta_{i_0,0} = d\cos\vartheta_{i_0,0}/\omega$ is the normalized AoD at the serving BS. Note that d denotes the distance between the antenna elements, ω is the signal wavelength, $\varphi_{i_0,0}$ is the physical AoA at u_0 and $\vartheta_{i_0,0}$ is the physical AoD at the serving BS. Note that $\phi_{i_0,0}$ and $\theta_{i_0,0}$ are assumed to follow the uniform distribution. The vector $\mathbf{a}_{N_B}(\theta_{i_0,0})$ can be written in a similar fashion.

The reflected channel denotes the channel between the typical user u_0 and its serving BS via a RIS, which consists of two components, i.e., the BS-RIS link and the RIS-user link. The channel for the BS-RIS link is first shown as

$$\mathbf{H}_{i_0,j_0} = \mathbf{a}_{N_R}(\phi_{i_0,j_0})\mathbf{a}_{N_B}^{\mathrm{H}}(\theta_{i_0,j_0}), \tag{4}$$

where ϕ_{i_0,j_0} and θ_{i_0,j_0} denote the normalized AoA at the associated RIS and the normalized AoD at the serving BS for the BS-RIS link. Similarly, the channel for the RIS-user link is

$$\mathbf{H}_{j_0,0} = \mathbf{a}_{N_U}(\phi_{j_0,0})\mathbf{a}_{N_R}^{\mathrm{H}}(\theta_{j_0,0}), \tag{5}$$

where $j_0 \in \Phi_R$ is the index of u_0's associated RIS, $\phi_{j_0,0}$ and $\theta_{j_0,0}$ denote the normalized AoA at u_0 and the normalized AoD at the associated RIS for the RIS-user link. Then, the

channel for the BS-user link via a RIS is

$$\mathbf{H}_{i_0,j_0,0} = \mathbf{H}_{j_0,0}\mathbf{\Psi}_{j_0}\mathbf{H}_{i_0,j_0}, \tag{6}$$

where $\mathbf{\Psi}_{j_0}$ is a diagonal matrix introduced by the RIS as

$$\mathbf{\Psi}_{j_0} = \text{diag}\{e^{j\psi_{1,j_0}}, \cdots, e^{j\psi_{N_R,j_0}}\}, \tag{7}$$

and $\psi_{n,j_0} \in [0, 2\pi), n = 1, \ldots, N_R$ is the phase shift introduced by the n-th element of the associated RIS of the typical user u_0.

Denote the beam directions that the serving BS and u_0 choose as θ_{i_0} and ϕ_0, respectively. The matched filter beamforming vectors are applied at the serving BS and u_0, which are shown as follows

$$\begin{cases} \mathbf{w}_0 = \mathbf{a}_{N_U}(\phi_0), \\ \mathbf{w}_{i_0} = \mathbf{a}_{N_B}(\theta_{i_0}). \end{cases} \tag{8}$$

Since the serving BS of u_0 may be LOS or NLOS, we adopt two different beamforming schemes for the LOS/NLOS cases. Specifically, (1) the RIS-oriented beamforming scheme is utilized when the serving BS is NLOS, which aims to optimize the reflected channel, i.e., $\phi_0 = \phi_{j_0,0}$ and $\theta_{i_0} = \theta_{i_0,j_0}$; (2) The user-oriented beamforming scheme is utilized when the serving BS is LOS, which aims to optimize the direct channel, i.e., $\phi_0 = \phi_{i_0,0}$ and $\theta_{i_0} = \theta_{i_0,0}$.

Based on the above assumptions, the received signal at u_0 is given in (9), as shown on the top of the next page, where s_0 is the transmitted signal from the serving BS to u_0, s_i is the transmitted signals from the interfering BSs to their associated users, $L_B(r_{i_0,0})$ is the path loss between u_0 and its serving BS, $L_R(r_{j_0,0})$ is the path loss between u_0 and its associated RIS, $L_{B,R}(r_{i_0,j_0})$ is the path loss between the associated RIS and the serving BS of u_0, $L_B(r_{i,0})$ is the path loss between u_0 and the interfering BS, $L_R(r_{j_0,0})$ is the path loss between u_0 and the interfering RIS, $L_{B,R}(r_{i_0,j_0})$ is the path loss between the interfering RIS and the interfering BS, $\mathbf{H}_{i,0}$ is the channel between u_0 and the interfering BS, $\mathbf{H}_{j,0}$ is the channel between u_0 and the interfering RIS, $\mathbf{w}_i$ is the beamforming vector of the interfering BS, $\mathbf{H}_{i,j}$ is the channel of the reflected link between the interfering BS and RIS, $\mathbf{\Psi}_j$ is the phase shift matrix of the interfering RIS, and $n_0 \sim \mathcal{CN}(0, \sigma^2)$ is the complex additive white Gaussian noise (AWGN).

III. Analysis of Meta Distribution

In this section, we first provide the statistical characterization of the path loss, then derive the meta distribution and energy efficiency of the RIS-assisted mmWave networks.

A. Auxiliary Results

In this subsection, we analyze the probability density function (PDF) and the CCDF of the distance between u_0 and its associated RIS.

Lemma 1: Given the distance between u_0 and its serving BS $r_{i_0,0}$, the distance between u_0 and its associated RIS $r_{j_0,0}$, and the angle between the RIS-user link and the BS-user link ϖ, the CCDF of the path loss between u_0 and its associated LOS/NLOS RIS providing a reflected link is given by

$$\bar{F}_{L_{R,E,\nu}}(x) = \mathbb{P}(L_{R,E,\nu} > x) = \exp(-\Lambda_{R,E,\nu}([0,x))), \tag{10}$$

where the intensity measures $\Lambda_{R,E,L}([0,x))$ and $\Lambda_{R,E,N}([0,x))$ are respectively given by

$$\begin{aligned} \Lambda_{R,E,L}([0,x)) = \lambda_R \int_{-\pi}^{\pi} \int_0^{(x/\kappa_L)^{1/\alpha_L}} \\ \mathcal{C}(r_{i_0,0}, r_{j_0,0}, \varpi) e^{-\beta r_{j_0,0}} r_{j_0,0} \mathrm{d}r_{j_0,0} \mathrm{d}\varpi, \end{aligned} \tag{11}$$

$$\begin{aligned} \Lambda_{R,E,N}([0,x)) = \lambda_R \int_{-\pi}^{\pi} \int_0^{(x/\kappa_L)^{1/\alpha_L}} \\ \mathcal{C}(r_{i_0,0}, r_{j_0,0}, \varpi) \left(1 - e^{-\beta r_{j_0,0}}\right) r_{j_0,0} \mathrm{d}r_{j_0,0} \mathrm{d}\varpi, \end{aligned} \tag{12}$$

$$\begin{aligned} &\mathcal{C}(r_{i_0,0}, r_{j_0,0}, \varpi) \\ &= \frac{1}{2} - \frac{1}{2\pi} \arccos\left(\frac{r_{j_0,0} - r_{i_0,0}\cos(\varpi)}{\sqrt{r_{i_0,0}^2 + r_{j_0,0}^2 - 2r_{i_0,0}r_{j_0,0}\cos(\varpi)}} \right). \end{aligned} \tag{13}$$

Proof: Please refer to [18].

The intensity measures for the RISs without the capability to provide a reflected link for u_0, i.e., $\Lambda_{R,NE,L}([0,x))$ and $\Lambda_{R,NE,N}([0,x))$, can be obtained following similar steps.

The probability that a RIS can provide a reflected link for u_0 and its serving BS at $r_{i_0,0}$ is

$$\begin{aligned} &\mathcal{C}(r_{j_0,0}) \\ &= 1 - \exp\left(-\lambda_B \int_{-\pi}^{\pi} \int_0^{\infty} \mathcal{C}(r_{i_0,0}, r_{j_0,0}, \varpi) r_{i_0,0} \mathrm{d}r_{i_0,0} \mathrm{d}\varpi \right). \end{aligned} \tag{14}$$

By averaging over $r_{j_0,0}$, the probability that a RIS can provide a reflected link for u_0 and its serving BS is can be obtained as

$$\begin{aligned} \mathcal{C} = \int_0^{\infty} \Lambda'_B([0,x)) \exp(-\Lambda_B([0,x))) \left(1 - \exp\left(-\lambda_B \right.\right. \\ \left.\left. \int_{-\pi}^{\pi} \int_0^{\infty} \mathcal{C}(r_{i_0,0}, r_{j_0,0}, \varpi) r_{i_0,0} \mathrm{d}r_{i_0,0} \mathrm{d}\varpi \right)\right) \mathrm{d}r_{j_0,0}. \end{aligned} \tag{15}$$

Due to the ergodicity of the point processes, the probability $\mathcal{C}$ can be regarded as the fraction of links with a assisting RIS. Then the utilization of the RISs is $\lambda_B \mathcal{C}/\lambda_R$.

Then the PDF of the path loss between u_0 and its associated LOS/NLOS RIS providing a reflected link is given by

$$\begin{aligned} f_{L_{R,E,\nu}} &= -\frac{d\bar{F}_{L_{R,E,\nu}}(x)}{\mathrm{d}x} \\ &= \Lambda'_{R,E,\nu}([0,x)) \exp(-\Lambda_{R,E,\nu}([0,x))), \end{aligned} \tag{16}$$

where

$$\begin{aligned} &\Lambda'_{R,E,L}([0,x)) = \\ &\frac{\lambda_R}{2} \int_{-\pi}^{\pi} \mathcal{C}(r_{i_0,0}, x, \varpi) e^{-\beta(x/\kappa_L)^{1/\alpha_L}} \alpha_L^{-1} \kappa_L^{-2/\alpha_L} x^{2/\alpha_L - 1} \mathrm{d}\varpi, \end{aligned} \tag{17}$$

$$R=\underbrace{\sqrt{P}\sqrt{L_B(r_{i_0,0})}\mathbf{w}_0^{\mathrm{H}}\mathbf{H}_{i_0,0}\mathbf{w}_{i_0}s_0+\sqrt{P}\sqrt{L_{B,R}(r_{i_0,j_0})L_R(r_{j_0,0})}\mathbf{w}_0^{\mathrm{H}}\mathbf{H}_{i_0,j_0,0}\mathbf{w}_{i_0}s_0}_{\text{desired signal}}+\underbrace{n_0}_{\text{noise}}$$
$$+\underbrace{\sum_{i\in\Phi_B}\sqrt{P}\sqrt{L_B(r_{i,0})}\mathbf{w}_0^{\mathrm{H}}\mathbf{H}_{i,0}\mathbf{w}_i s_i+\sum_{j\in\Phi_R}\sqrt{P}\sqrt{L_R(r_{j,0})}\mathbf{w}_0^{\mathrm{H}}\mathbf{H}_{j,0}\mathbf{\Psi}_j\sum_{i\in\bar{\Phi}_B}\sqrt{L_{B,R}(r_{i,j})}\mathbf{H}_{i,j}\mathbf{w}_i s_i}_{\text{interference}}. \tag{9}$$

$$\Lambda'_{R,E,N}([0,x))=\frac{\lambda_R}{2}\int_{-\pi}^{\pi}\mathcal{C}(r_{i_0,0},x,\varpi)\left(1-e^{-\beta(x/\kappa_L)^{1/\alpha_L}}\right)\alpha_L^{-1}\kappa_L^{-2/\alpha_L}x^{2/\alpha_L-1}\mathrm{d}\varpi. \tag{18}$$

B. Meta Distribution

In this subsection, we first analyze the moments of the conditional success probability. According to the LOS/NLOS link state, the interference experienced by u_0 are from four sets, i.e., the set of LOS BSs $\Phi_{B,L}$, the set of LOS BSs $\Phi_{B,N}$, the set of LOS RISs with $\Phi_{R,L}$ and the set of NLOS RISs $\Phi_{R,N}$. By carefully handling the interference from the two sets, the k-th moment of the conditional success probability can be derived utilizing the law of total probability in the following theorem.

Theorem 1: The k-th moment of the conditional success probability in a RIS-assisted mmWave network is given by

$$M_k=\mathcal{C}M_{k,E}+(1-\mathcal{C})M_{k,NE}, \tag{19}$$

$$M_{k,E}=\frac{1}{2\pi}\sum_{\rho\in\{L,N\}}\sum_{\nu\in\{L,N\}}\int_0^{2\pi}\int_0^{\infty}\int_0^{\infty}\int_{-\frac{d}{\omega}}^{\frac{d}{\omega}}\int_{-\frac{d}{\omega}}^{\frac{d}{\omega}}\sum_{\tau_1=0}^{\infty}\sum_{\tau_2=0}^{W\tau_1}\binom{k}{\tau_1}\binom{W\tau_1}{\tau_2}(-1)^{\tau_1+\tau_2}e^{-s\sigma^2}\mathcal{L}_{I_B}(s_{B,\rho})\mathcal{L}_{I_R}(s_{R,\rho})f_{L_{B,\rho}}(l_{B,\rho})f_{L_{R,E,\nu}}(l_{R,E,\nu})\mathrm{d}\theta_{S_\rho}\mathrm{d}\phi_{S_\rho}\mathrm{d}l_{B,\rho}\mathrm{d}l_{R,E,\nu}\mathrm{d}\varpi, \tag{20}$$

$$M_{k,NE}=\sum_{\rho\in\{L,N\}}\int_0^{\infty}\sum_{\tau_1=0}^{\infty}\sum_{\tau_2=0}^{W\tau_1}\binom{k}{\tau_1}\binom{W\tau_1}{\tau_2}(-1)^{\tau_1+\tau_2}e^{-s\sigma^2}\mathcal{L}_{I_B}(s_{B,L})f_{L_{B,\rho}}(l_{B,\rho})\mathrm{d}l_{B,\rho}, \tag{21}$$

where $s_{B,\rho}=\tau_2(W\tau_1)((W\tau_1)!)^{\frac{1}{W\tau_1}}TS_{B,\rho}^{-1}$, $s_{R,\rho}=\tau_2(W\tau_1)((W\tau_1)!)^{\frac{1}{W\tau_1}}TS_{R,\rho}^{-1}$.

Proof: See Appendix.

Note that the computation of the k-th moment of the conditional success probability, i.e., M_k, can be divided into two cases. When the reflected link exists, the user-oriented or RIS-oriented beamforming scheme is adopted according to the link state between u_0 and its serving BS. When the reflected link does not exist, the user-oriented beamforming scheme is adopted. M_k is dependent on the physical layer parameters, i.e., the densities of the BSs and the RISs, transmit powers and the path loss exponents and the size of the RISs. The randomness of the interference stems from three components, i.e., the beam orientations, RIS orientations, BS and blockage locations.

By applying the Gil-Pelaez theorem, the meta distribution of the SINR is

$$\bar{F}_{\mathcal{P}}(x)=\frac{1}{2}+\frac{1}{\pi}\int_0^{\infty}\frac{\mathcal{J}\left(e^{-jt\log x}M_{jt}\right)}{t}\mathrm{d}t, \tag{22}$$

where M_{jt} can be obtained by replacing k with jt in (23), while $\mathcal{J}(z)$ is the imaginary part of z.

From Theorem 1, we can also observe that the k-th moment of the conditional success probability is not in closed-form and it is difficult to obtain the analytically tractable results. To facilitate the computation process, the Gauss-Chebyshev quadrature (GCQ) formula [19] can be utilized to compute the success probability.

C. Analysis of Area Spectral Efficiency and Energy Efficiency

In this subsection, we first derive the mean local delay, then provide expression of the ASE and energy efficiency.

Theorem 2: The mean local delay of a RIS-assisted mmWave network is given by

$$M_{-1}=\mathcal{C}M_{-1,E}+(1-\mathcal{C})M_{-1,NE}, \tag{23}$$

where

$$M_{-1,E}=\frac{1}{2\pi}\sum_{\rho\in\{L,N\}}\sum_{\nu\in\{L,N\}}\int_0^{2\pi}\int_0^{\infty}\int_0^{\infty}\int_{-\frac{d}{\omega}}^{\frac{d}{\omega}}\int_{-\frac{d}{\omega}}^{\frac{d}{\omega}}\sum_{\tau_1=0}^{\infty}\sum_{\tau_2=0}^{W\tau_1}\binom{W\tau_1}{\tau_2}(-1)^{\tau_2}e^{-s\sigma^2}\mathcal{L}_{I_B}(s_{B,\rho})\mathcal{L}_{I_R}(s_{R,\rho})f_{L_{B,\rho}}(l_{B,\rho})f_{L_{R,E,\nu}}(l_{R,E,\nu})\mathrm{d}\theta_{S_\rho}\mathrm{d}\phi_{S_\rho}\mathrm{d}l_{B,\rho}\mathrm{d}l_{R,E,\nu}\mathrm{d}\varpi, \tag{24}$$

$$M_{-1,NE}=\sum_{\rho\in\{L,N\}}\int_0^{\infty}\sum_{\tau_1=0}^{\infty}\sum_{\tau_2=0}^{W\tau_1}\binom{W\tau_1}{\tau_2}(-1)^{\tau_2}e^{-s\sigma^2}\mathcal{L}_{I_B}(s_{B,L})f_{L_{B,\rho}}(l_{B,\rho})\mathrm{d}l_{B,\rho}. \tag{25}$$

The ASE is defined as the average number of successfully transmitted nats per second per hertz per unit area, which is given by

$$\mathrm{ASE}=\mathcal{C}\frac{\lambda_B\log(1+T)}{M_{-1,E}}+(1-\mathcal{C})\frac{\lambda_B\log(1+T)}{M_{-1,NE}}. \tag{26}$$

In practice, a main proportion of the energy for cellular networks is consumed by the BSs. The total BS power consumption consists of two components: the static power consumption and the transmit power. Henceforth, a linear approximation model has been widely employed to describe the power consumption, i.e., $P_{tot} = P_0 + \Delta P$, where $1/\Delta$ denotes the power amplifier efficiency, P the transmit power and P_0 the static circuit power consumption. Let P_e be the power consumption of each element in RIS, the energy efficiency is then defined as the ratio of the ASE and the corresponding average power consumption:

$$\mathrm{EE} = \frac{\mathrm{ASE}}{\lambda_B P_{tot} + (\lambda_R - \lambda_B \mathcal{C}) N_R P_e}. \tag{27}$$

IV. Simulation Results

In this section, we consider a RIS-assisted mmWave cellular network. We present the impact of the key network parameters on the meta distribution, success probability, variance of the conditional success probability, ASE and energy efficiency. The tradeoff between the BS and RIS density is also investigated. Unless otherwise stated, the parameters are set as listed in the following table.

Table I
System Parameters

Parameters	Values
BS transmit power	$P_B = 33$dBm
BS static power consumption	$P_0 = 10W$
Efficiency of power amplifier	$1/\Delta = 1/6$
Number of antennas in BS	$N_B = 8$
Number of antennas in user	$N_U = 4$
Number of elements in RIS	$N_R = 128$
Power consumption of each element in RIS	$P_e = 7$dBm
Path loss exponent	$\alpha_L = 2$, $\alpha_N = 4$
BS density	$\lambda_B = 10/(500^2\pi)$
RIS density	$\lambda_R = 60/(500^2\pi)$
User density	$\lambda_U = 100/(500^2\pi)$
Blockage parameter	$\beta_1 = 0.01$
Carrier frequency	28GHz
Path loss intercept	$C_L = C_N = (F_c/4\pi)^2$
Noise figure	10dB
Noise power	-174dBm/Hz+10log$_{10}$W +10dB

Fig. 2 plots the meta distribution against y. The fraction of users with conditional STP values around y can be reflected by the slope of the meta distribution with respect to y. A larger slope corresponds to a larger fraction of users with conditional success probability values around y and vice versa. Compared to mmWave networks without RISs, given an arbitrary percentage y, a larger fraction of users in the mmWave network with RISs achieve the success probability larger than y, which indicates that the introduction of the RISs increases the success probability. In addition, the cell-edge success probability increases due to the deployment of the RISs, which indicates that the deployment of the RISs can boost up the cell-edge rate.

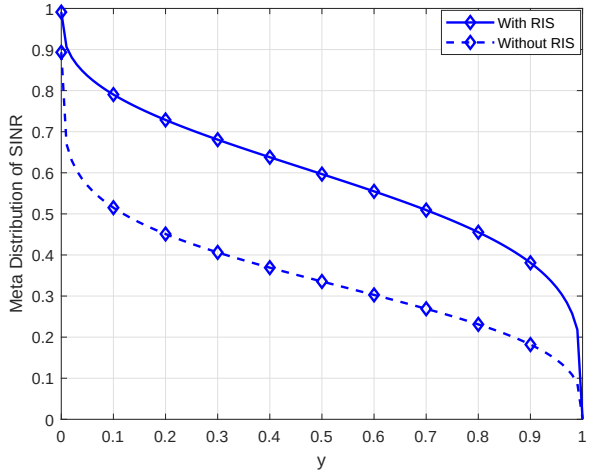

Figure 2. Meta distribution as a function of the SINR threshold.

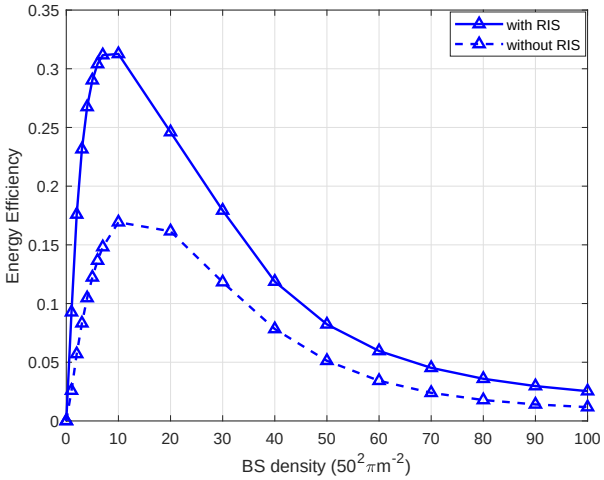

Figure 3. Energy efficiency as a function of BS density.

Fig. 3 illustrates the energy efficiency as a function of the BS density. We can observe that the energy efficiency decreases more rapidly than the ASE. This can be explained as follows. When the BS density is relatively small, the energy efficiency increases since the success probability increases. However, when the BS density further increases, the increasing power consumption and the decreasing success probability contributes to the reduction of the energy efficiency. In addition, the results show that introducing RISs into cellular networks can efficiently improve the energy efficiency of the dense cellular networks.

V. Conclusion

We have developed a meta distribution-based framework to investigate the performance of a RIS-assisted mmWave

network. By considering the orientation of the RISs, we have provided a statistical characterization of the path loss of the RISs and derived the expression of the RIS utilization. We have derived analytical expressions for the moments of the conditional success probability and the mean local delay when the reflected link exists or does not exist. Accordingly, the expressions of the area spectral efficiency and the energy efficiency were derived. Numerical results have demonstrated that the RISs supplement significantly mmWave networks without RISs and can efficiently improve the success probability with limited power consumption.

APPENDIX

Given that the reflected link exists, the k-th moment of the conditional success probability can be derived as follows

$$M_{k,E} = \mathbb{P}(\text{SINR}_\rho > T|\Phi) = \mathbb{P}\left(\frac{S_{B,\rho}+S_{R,\rho}}{I_B+I_R+\sigma^2} > T\right)^k$$

$$=\mathbb{P}\left(1 > \frac{T\left(I_B+I_R+\sigma^2\right)}{S_{B,\rho}+S_{R,\rho}}\right)^k$$

$$\overset{(a)}{\approx} \frac{1}{A_R}\mathbb{P}\left(\nu > \frac{T\left(I_B+I_R+\sigma^2\right)}{S_{B,\rho}+S_{R,\rho}}\right)^k$$

$$\overset{(b)}{\approx} \frac{1}{A_R}\mathbb{E}_{I,s}\left[\left(\frac{\Gamma(W,s(\sigma^2+I))}{\Gamma(W)}\right)^k\right]$$

$$\overset{(c)}{=} \frac{1}{A_R}\mathbb{E}_{\theta_{i_0,j_0},\phi_{S_\rho},\theta_{S_\rho},r_{i_0,0},r_{j_0,0},\varpi}\left[\sum_{\rho\in\{L,N\}}\sum_{\nu\in\{L,N\}}\sum_{\tau_1=0}^{\infty}\sum_{\tau_2=0}^{W\tau_1}\right.$$
$$\left.\binom{k}{\tau_1}\binom{W\tau_1}{\tau_2}(-1)^{\tau_1+\tau_2}e^{-s\sigma^2}\mathcal{L}_{I_B}(s)\mathcal{L}_{I_R}(s)\right]$$

$$\overset{(d)}{=} \frac{1}{2\pi A_R}\sum_{\rho\in\{L,N\}}\sum_{\nu\in\{L,N\}}\int_0^{2\pi}\int_0^{\infty}\int_0^{\infty}\int_{-\frac{d}{\omega}}^{\frac{d}{\omega}}\int_{-\frac{d}{\omega}}^{\frac{d}{\omega}}\sum_{\tau_1=0}^{\infty}\sum_{\tau_2=0}^{W\tau_1}$$
$$\binom{k}{\tau_1}\binom{W\tau_1}{\tau_2}(-1)^{\tau_1+\tau_2}e^{-s\sigma^2}\mathcal{L}_{I_B}(s_{B_\rho})\mathcal{L}_{I_R}(s_{R_\rho})$$
$$f_{L_{B,\rho}}(l_{B,\rho})f_{L_{R,E,\nu}}(l_{R,E,\nu})\mathrm{d}\theta_{S_\rho}\mathrm{d}\phi_{S_\rho}\mathrm{d}l_{B,\rho}\mathrm{d}l_{R,E,\nu}\mathrm{d}\varpi,$$

where (a) follows from that a "dummy" gamma variable ν with shape parameter W and unit mean is utilized to approximate the constant number one and ν converges to one when W geoes to infinity, i.e., $\lim_{w\to\infty}\frac{w^w x^{w-1}e^{-wx}}{\Gamma(w)} = \delta(x-1)$ [20], where $\delta(x)$ is the Dirac delta function; (b) is from Alzer's inequality [21]; (c) follows from the binomial theorem and the independence between $I_{BS,L}$, $I_{BS,N}$, $I_{R,L}$ and $I_{R,N}$; (d) follows from the PDF of the distance between u_0 and its serving BS/RIS. Note that $M_{k,NE}$ can be derived following similar steps to the derivation of $M_{k,E}$.

REFERENCES

[1] M. Xiao *et al.*, "Millimeter wave communications for future mobile networks," *IEEE J. Sel. Areas Commun.*, vol. 35, no. 9, pp. 1909-1935, Sept. 2017.

[2] J. Zhang, E. Björnson, M. Matthaiou, D. W. K. Ng, H. Yang, and D. J. Love, "Prospective multiple antenna technologies for beyond 5G," *IEEE J. Sel. Areas Commun.*, vol. 38, no. 8, pp. 1637-1660, Aug. 2020.

[3] W. Tang *et al.*, "Wireless communications with reconfigurable intelligent surface: Path loss modeling and experimental measurement," *IEEE Trans. Wireless Commun.*, vol. 20, no. 1, pp. 421-439, Jan. 2021.

[4] W. Tang *et al.*, "MIMO transmission through reconfigurable intelligent surface: System design, analysis, and implementation," *IEEE J. Sel. Areas Commun.*, vol. 38, no. 11, pp. 2683-2699, Nov. 2020.

[5] E. Björnson, Ö. Özdogan and E. G. Larsson, "Intelligent reflecting surface versus decode-and-forward: how large surfaces are needed to beat relaying?" *IEEE Wireless Commun. Letters*, vol. 9, no. 2, pp. 244-248, Feb. 2020.

[6] K. Feng, X. Li, Y. Han, S. Jin, and Y.-J. Chen, "Physical layer security enhancement exploiting intelligent reflecting surface," *IEEE Commun. Letters*, vol. 25, no. 3, pp. 734-738, Mar. 2021.

[7] O. Yurduseven, S. D. Assimonis, and M. Matthaiou, "Intelligent reflecting surfaces with spatial modulation: An electromagnetic perspective," *IEEE Open J. Commun. Soc.*, vol. 1, pp. 1256-1266, Sep. 2020.

[8] X. Yu, D. Xu, and R. Schober, "Enabling secure wireless communications via intelligent reflecting surfaces," in *Proc. IEEE GLOBECOM*, Dec. 2019.

[9] X. Guan, Q. Wu, and R. Zhang, "Intelligent reflecting surface assisted secrecy communication: Is artificial noise helpful or not?" *IEEE Wireless Commun. Letters*, vol. 9, no. 6, pp. 778-782, Jun. 2020.

[10] J. Chen, Y.-C. Liang, Y. Pei, and H. Guo, "Intelligent reflecting surface: a programmable wireless environment for physical layer Security," *IEEE Access*, vol. 7, pp. 82599-82612, Jun. 2019.

[11] Y. Zhu, G. Zheng, and K.-K.Wong, "Stochastic geometry anaylsis of large intelligent surface-assisted millimeter networks," *IEEE J. Sel. Areas Commun.*, vol. 38, no. 8, pp. 1749-1762, Aug. 2020.

[12] M. A. Kishk and M.-S. Alouini, "Exploiting randomly-located blockages for large-scale deployment of intelligent surfaces," *IEEE J. Sel. Areas Commun.*, vol. 39, no. 4, pp. 1043-1056, Apr. 2021.

[13] M. Haenggi, "The meta distribution of the SIR in Poisson bipolar and cellular networks," *IEEE Trans. Wireless Commun.*, vol. 15, no. 4, pp. 2577-2589, Apr. 2016.

[14] T. Bai and R. W. Heath, Jr., "Coverage and rate analysis for millimeter-wave cellular networks," *IEEE Trans. Wireless Commun.*, vol. 14, no. 2, pp. 1100-1114, Feb. 2015.

[15] S. Sun, T. Rappaport, R. W. Heath, Jr., A. Nix, and S. Rangan, "MIMO for millimeter-wave wireless communications: Beamforming, spatial multiplexing, or both?" *IEEE Commun. Mag.*, vol. 52, no. 12, pp. 110-121, Dec. 2014.

[16] Z. Xiao, T. He, P. Xia, and X.-G. Xia, "Hierarchical codebook design for beamforming training in millimeter-wave communication," *IEEE Trans. Wireless Commun.*, vol. 15, no. 5, pp. 3380-3392, May 2016.

[17] T. S. Rappaport, F. Gutierrez, E. Ben-Dor, J. N. Murdock, Y. Qiao, and J. I. Tamir, "Broadband millimeter-wave propagation measurements and models using adaptive-beam antennas for outdoor urban cellular communications," *IEEE Trans. Antennas Propag.*, vol. 61, no. 4, pp. 1850-1859, Apr. 2013.

[18] L. Yang, F.-C. Zheng, and S. Jin, "Coverage probability and energy efficiency of reconfigurable intelligent surface-assisted mmWave networks," 2021, *arXiv:2104.07971*. [Online]. Available: http://arxiv.org/abs/2104.07971.

[19] M. Abramowitz and I. A. Stegun, *Handbook of Mathematical Functions with Formulas, Graphs, and Mathematical Tables*, 9th ed. New York, USA: Dover Publications, 1972.

[20] R. Aris, *Mathematical Modeling: A Chemical Engineers Perspective*. San Diego, CA, USA: Academic, 1999.

[21] H. Alzer, "On some inequalities for the incomplete gamma function," *Math. Comput.*, vol. 66, pp. 771-778, Apr. 1997.